Cellular Microbiology (2015) **17**(8), 1133–1143
doi:10.1111/cmi.12424
First published online 15 February 2015

Translocation of botulinum neurotoxin serotype A and associated proteins across the intestinal epithelia

Tina I. Lam,[1] Larry H. Stanker,[1] Kwangkook Lee,[2] Rongsheng Jin[2] and Luisa W. Cheng[1]*

[1]*Foodborne Toxin Detection and Prevention Unit, Western Regional Research Center, U.S. Department of Agriculture -Agricultural Research Service, Albany, CA 94710, USA.*

[2]*Physiology & Biophysics, School of Medicine, University of California, Irvine, CA 92697, USA.*

Summary

Botulinum neurotoxins (BoNTs) are some of the most poisonous natural toxins. Botulinum neurotoxins associate with neurotoxin-associated proteins (NAPs) forming large complexes that are protected from the harsh environment of the gastrointestinal tract. However, it is still unclear how BoNT complexes as large as 900 kDa traverse the epithelial barrier and what role NAPs play in toxin translocation. In this study, we examined the transit of BoNT serotype A (BoNT/A) holotoxin, complex and recombinantly purified NAP complex through cultured and polarized Caco-2 cells and, for the first time, in the small mouse intestine. Botulinum neurotoxin serotype A and NAPs in the toxin complex were detectable inside intestinal cells beginning at 2 h post intoxication. Appearance of the BoNT/A holotoxin signal was slower, with detection starting at 4–6 h. This indicated that the holotoxin alone was sufficient for entry but the presence of NAPs enhanced the rate of entry. Botulinum neurotoxin serotype A detection peaked at approximately 6 and 8 h for complex and holotoxin, respectively, and thereafter began to disperse with some toxin remaining in the epithelia after 24 h. Purified HA complexes alone were also internalized and followed a similar time course to that of BoNT/A complex internalization. However, recombinant HA complexes did not enhance BoNT/A holotoxin entry in the absence of a physical link with BoNT/A. We propose a model for BoNT/A toxin complex translocation whereby toxin complex entry is facilitated by NAPs in a receptor-mediated mechanism. Understanding the intestinal uptake of BoNT complexes will aid the development of new measures to prevent or treat oral intoxications.

Received 10 June, 2014; revised 18 December, 2014; accepted 15 January, 2015. *For correspondence. E-mail luisa.cheng@ars.usda.gov; Tel. (+1) 510 559 6337; Fax (+1) 510 559 5880.

Introduction

Botulinum neurotoxins (BoNTs) are produced by gram-positive, anaerobic, spore-forming *Clostridium* species (Arnon *et al.*, 2001). Seven different botulinum serotypes (A–G) have been identified thus far with a possible eight serotype H recently reported and awaiting further characterization (Barash and Arnon, 2014). They are among the most toxic substances to humans and are the causative agents of botulism. Most foodborne intoxications are caused by BoNT serotypes A, B, E and occasionally by serotype F (Arnon *et al.*, 2001; Bigalke and Rummel, 2005; Scarlatos *et al.*, 2005). BoNTs are synthesized as ~150 kDa holotoxins, which like other A-B dimeric toxins consist of two polypeptides, an ~100 kDa heavy chain and an ~50 kDa light chain, linked by a single disulfide bond. Botulinum neurotoxins specifically target the peripheral cholinergic neurons, where they cleave proteins associated with intracellular vesicular transport, such as SNAP-25 (synaptosomal-associated protein of 25 kDa), VAMP (vesicle-associated membrane protein) or syntaxin (Schiavo *et al.*, 1993; Montecucco and Schiavo, 1994; Montecucco *et al.*, 1996). Cleavage of these proteins leads to the inhibition of acetylcholine release from neurons, causing flaccid muscle paralysis.

Clostridia spp. secreted BoNT holotoxins along with non-toxic neurotoxin-associated proteins (NAPs) to form large toxin complexes known as 'progenitor' toxin complexes (Ohishi *et al.*, 1977; Inoue *et al.*, 1996; Hines *et al.*, 2005; Eisele *et al.*, 2011). Botulinum neurotoxin complexes of different sizes are also known as 12S, 16S or 19S complexes, with molecular sizes of approximately 300, 500 and 900 kDa, respectively. The 12S complex of botulinum neurotoxin serotype A (BoNT/A) is composed of BoNT/A holotoxin and the non-toxic, non-haemagglutinin (NTNH) protein; the 16S is composed of NTNH and different haemagglutinin proteins (consisting of HA70, HA33

and HA17); and the 19S is presumably composed of a dimer of the 16S complex.

In foodborne botulism, BoNT must cross intestinal epithelial barriers to enter the blood stream and reach target neurons. The mechanism of how the large BoNT holotoxin or its multi-subunit complexes traverse the polarized epithelial monolayer is not fully understood. The three-dimensional structure of the BoNT/A complex has recently been elucidated (Gu *et al*., 2012; Lee *et al*., 2013). Carbohydrate binding sites have been identified and recently shown to be involved in binding to intestinal epithelia. BoNT holotoxins are known to cross the intestinal epithelium from the apical side and relocate to the basolateral side via transcytosis (Maksymowych and Simpson, 1998; 2004; Ahsan *et al*., 2005; Fujinaga *et al*., 2009; Fujinaga, 2010). Large BoNT complexes have been shown to increase oral toxicity in mice by about 20 times over that of purified holotoxin. Toxin complex size is directly proportional to oral toxicity: the larger the complex, the greater the oral toxicity (Ohishi *et al*., 1977; Sugii *et al*., 1977; Chen *et al*., 1998). Studies by others suggest an active role for the NAPs, such as HA33 binding to surface receptors followed by internalization and transcytosis. HA33 was shown to disrupt epithelial tight junctions from the basolateral side, promoting rapid toxin complex passage via a paracellular mechanism (Fujinaga *et al*., 2009; Jin *et al*., 2009).

There are at least two proposed mechanisms of BoNT translocation. The first purports that NAPs only protect BoNTs from the low pH and degradative effects of intestinal juices and play no role in holotoxin uptake. In this model, BoNT holotoxin alone is able to traverse the intestinal and lung epithelium and reach the bloodstream intact (Maksymowych *et al*., 1999; Ahsan *et al*., 2005; Al-Saleem *et al*., 2012; Couesnon *et al*., 2012; Simpson, 2013). In a second model, NAPs play a direct function in binding intestinal receptors, disrupting tight junctions in the intestinal epithelial cell barrier, and promoting the paracellular transport of BoNTs following initial transcytosis (Matsumura *et al*., 2008; Jin *et al*., 2009; Sugawara *et al*., 2010). However, most of the evidence supporting either hypothesis is derived from *in vitro* cultured intestinal cell models and limited *ex vivo* studies that do not provide a complete picture of how toxin complexes translocate across the intestinal epithelia.

Despite vast studies on BoNT, three fundamental questions remain to be answered. First, given its unusually large size (~ 900 kDa), how does a toxin complex (holotoxin plus NAPs) translocate across the intestinal epithelium? Second, does this large complex remain intact once inside the intestinal epithelium? Third, what role do NAPs play in oral intoxication? We utilized multiple approaches to address these questions, including polarized membranes and both *in vitro* and *in vivo* methods. Comparing the findings from these different experimental methods has now allowed us to propose a model of BoNT intestinal translocation.

Results

Uptake of BoNT/A and NAPs into cultured intestinal epithelial cells

Purified BoNT/A complex is composed of the 150 kDa holotoxin (about 30% of total weight), the NTNH (140 kDa) and the HA complex (HA-C) of about 470 kDa which includes HA70, HA33 and HA17 (Supporting Information Fig. S1) (Cheng *et al*., 2008). To compare the internalization of each component of the toxin complex, we first used Caco-2, human colon adenocarcinoma cells as the *in vitro* model. Cells were grown in tissue culture media at 37°C at neutral pH and were treated with 50 ng/well of the BoNT/A complex (AC), 15 ng/well of the BoNT/A holotoxin (AHT) or with 20 ng/well of HA-C for 4 h. Immunofluorescence staining with the rabbit anti-BoNT/A antibodies showed the presence of BoNT/A complex and holotoxin throughout the depth of Caco-2 cells after 4 h of incubation, indicating internalization of toxins from the surface of cells to the cytosol (Fig. 1, Supporting Information Figs S2 and S3). Labelled mAb against HA70 revealed internalization of HA70 in both the BoNT/A complex and the HA-C after 4 h. Probing with the NTNH monoclonal antibody showed internalization of NTNH only in the BoNT/A complex, as NTNH is not present in the HA-C. The signal intensities for BoNT/A, HA70 and NTNH in the immunofluorescence images were quantified with ImageJ for comparison (Fig. 1B–D). A 63× magnification view of Caco-2 cells treated with either BoNT/A holotoxin or complex showed the presence of BoNT/A labelled vesicles indicative of cellular transcytosis (Supporting Information Fig. S4).

The Caco-2 cell culture assay allowed us to measure the temporal pattern of toxin binding, internalization, and location of toxin and NAPs. We treated Caco-2 cells with BoNT/A in the presence or absence of NAPs for 1 h followed by washes with media to remove unbound material. We then monitored cellular uptake of BoNT/A over the course of 8 h. Caco-2 cells exposed to 50 ng BoNT/A complex showed that cell binding and internalization occurred starting approximately 2 h and peaked at 6 h (Fig. 2A). Immunofluorescence signals for the associated proteins showed that HA70 and NTNH cellular binding and internalization occurred at the same time as the BoNT/A holotoxin (Fig. 2A). In the absence of NAPs, BoNT/A signal appeared later than the BoNT/A complex in the Caco-2 cells. Beginning at 2 h, less BoNT/A staining is observed in the holotoxin-treated vs. complex-treated cells (Fig. 2B). The signal difference however is not

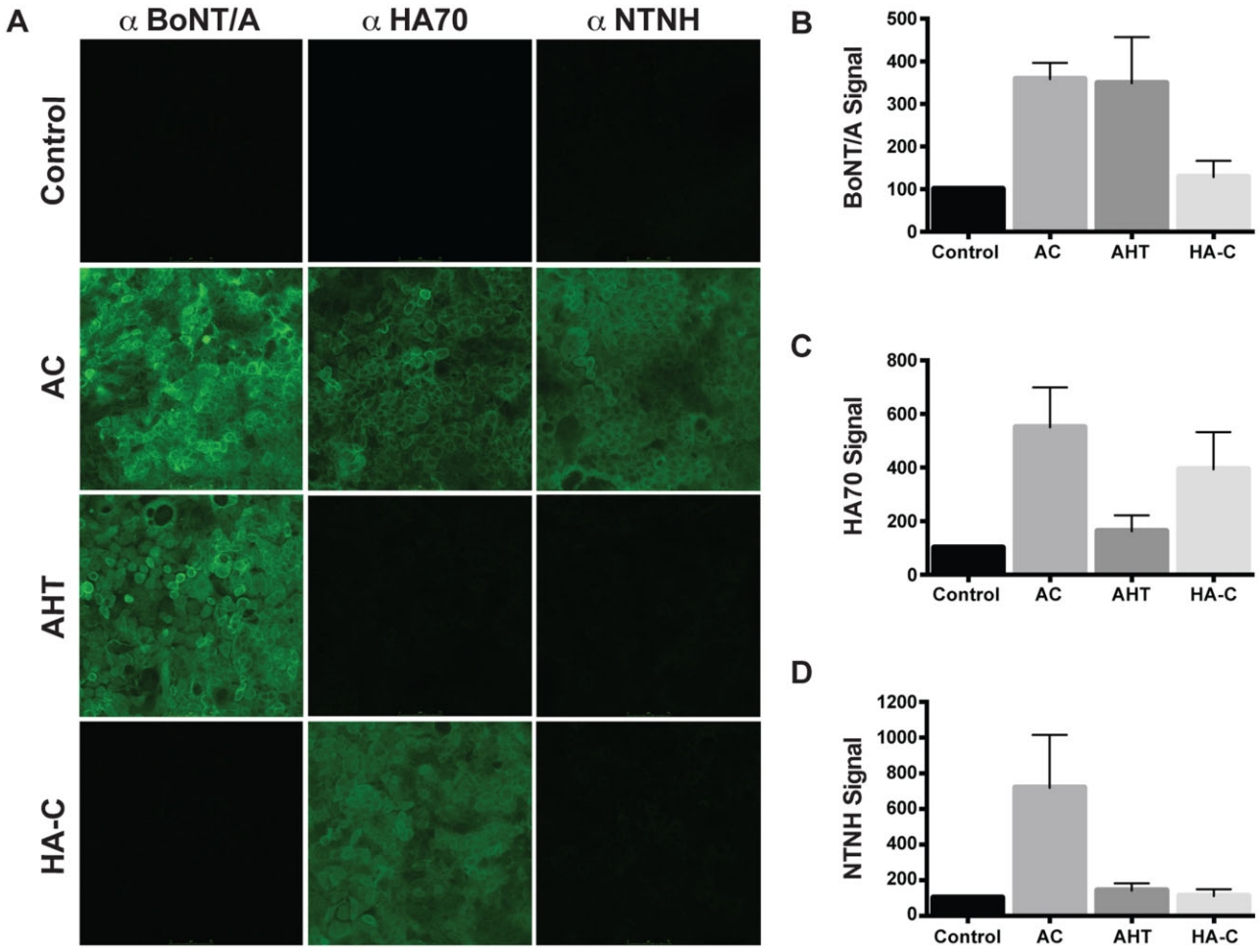

Fig. 1. Internalization of BoNT/A holotoxin, BoNT/A complex and NAPs (HA70 and NTNH) into Caco-2 cells.
A. Caco-2 cells were treated with media (control) or with BoNT/A complex (AC), holotoxin (AHT) or recombinant HA complex (HA-C) for 4 h at 37°C. Cells were stained with of Alexa-488 labelled antibodies against BoNT/A, HA70 and NTNH. The fluorescence signals for BoNT/A, HA70 and NTNH were quantitated by determining mean fluorescence from Caco-2 cells from three randomly chosen optical fields from each of four to five coverslips per experiment using ImageJ software (B–D). Values represent means of four independent experiments ± SEM.

statistically significant until 6 h after adding the toxin. There was minimal background HA70 or NTNH immunofluorescence signal as expected. Furthermore, we confirmed that the HA-C could bind Caco-2 cells independently of BoNT/A holotoxin. Anti-HA70 immunofluorescence from cells treated with the HA-C showed a similar binding and internalization pattern as that of the HA70 signal associated with the BoNT/A complex (Fig. 2C). When BoNT/A holotoxin was added to Caco-2 cells along with the recombinant HA-C, binding and internalization of BoNT/A resembled that of holotoxin alone. Thus, in the absence of a physical interaction between the holotoxin and HA-C through NTNH, the HA-C did not enhance holotoxin entry (Fig. 2D). The internalization of BoNT and NAPs into the Caco-2 cells was visualized in Z stacked images of the labelled cells (Supporting Information Fig. S2). Caco-2 cells were labelled with fluorescence-labelled BoNT/A throughout the depth of cells and showed the typical ringed labelling where there is nuclei exclusion and presence of toxin-labelled vesicles (Supporting Information Figs S2 and S4). This significant difference in the temporal pattern of binding indicates that NAPs reduced the amount of time needed to cross epithelia perhaps by actively promoting receptor binding and presumably carrying the holotoxin inside.

Effect of BoNT/A and NAPs on transepithelial membrane integrity

HA33, a component of the HA-C, was previously shown to disrupt membrane tight junctions (Fujinaga *et al*., 2009; Jin *et al*., 2009). However, these studies utilized unusual growth conditions such as low temperatures as well as very large amounts of toxins. To determine the effect of

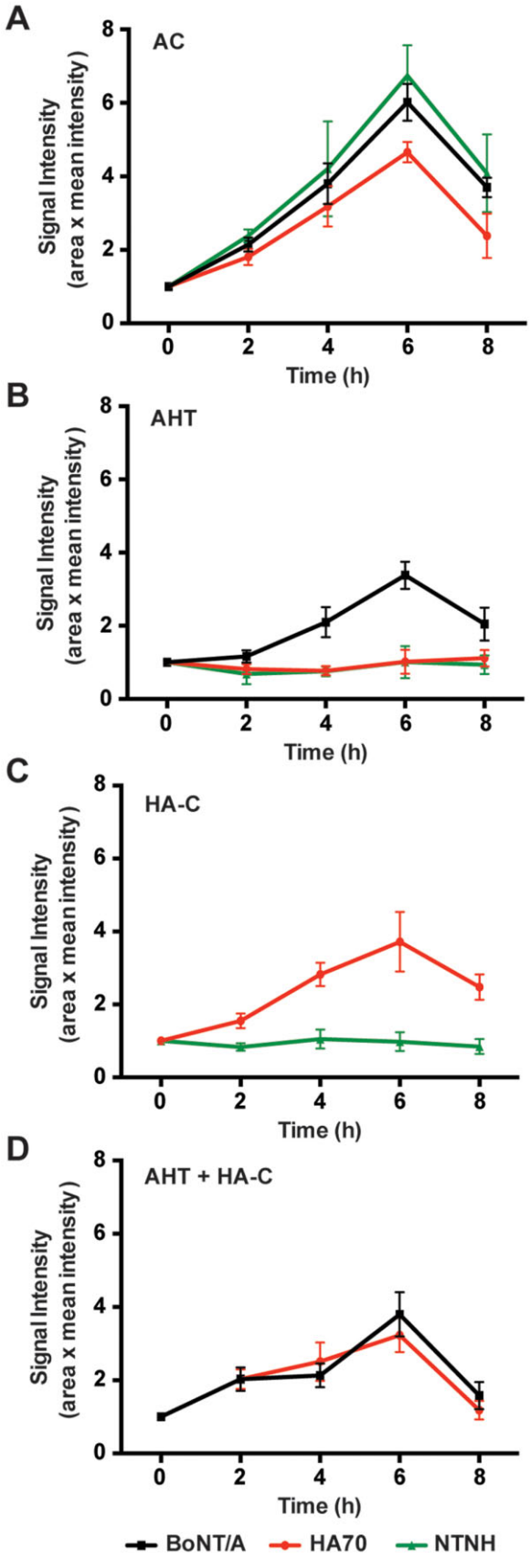

Fig. 2. Time-dependent binding and internalization of BoNT/A, HA70 and NTNH in Caco-2 cells. Caco-2 cells were treated with 50 ng of the BoNT/A complex (A), 15 ng of BoNT/A holotoxin (B), 20 ng of HA complex (C), or 15 ng BoNT/A holotoxin and 20 ng of HA complex (D) for 1 h. The cellular uptake of BoNT/A, HA70 and NTNH was measured by quantifying their immunofluorescence signal over time. Each data point represents the mean of four independent experiments ± SEM.

BoNT on epithelial cell membrane integrity and the role of the HA-C, we cultured polarized epithelial cells in transwells and measured the transepithelial electrical resistance (TER). A decrease in TER indicates a disruption in tight junctions. We applied either the BoNT/A holotoxin, the toxin complex, or the HA-C alone, or in combination with holotoxin, to the apical sides and measured TER values at 37°C under neutral pH over a period of 24 h. When polarized Caco-2 cells were treated with either the BoNT/A complex or the HA-C, the TER value dropped to approximately 55% after 10 h of exposure. This change in TER indicated a slight disruption of tight junctions as compared with the control, Hank's Balanced Salt Solution (HBSS) or following treatment with BoNT/A holotoxin, where the TER dropped to approximately 86% after 10 h (Fig. 3A). No significant differences in TER values were observed in Caco-2 cells exposed to the holotoxin or the control media (Fig. 3A). Surprisingly, when Caco-2 cells were exposed basolaterally to the BoNT/A complex and HA-C, only a small decrease in TER value to 70% was observed. Likewise, a small decrease in TER to approximately 80% following exposure to BoNT/A holotoxin was observed, indicating minimal disruption of tight junctions (Fig. 3B). We also tested TER on cells treated with BoNT/A complex under acidic pH (pH 6.0) but did not observe any significant differences (data not shown).

In vivo *translocation of BoNT/A complex, holotoxin or HA-C through the mouse small intestinal villi*

Little is known regarding the fate of BoNT once ingested. Previous studies have used *ex vivo* models or ligated intestines to examine the effects of exposure to recombinant BoNT complexes or fragments of BoNTs (Couesnon *et al.*, 2012; Lee *et al.*, 2014). Here we used the mouse oral model of intoxication to study the translocation of the native BoNT/A holotoxin, the BoNT/A complex and the recombinant HA-C. Passages of BoNT and NAPs through the small intestine were tracked over 24 h (Figs 4 and 5 and Supporting Information Fig. S5). Similar to the *in vitro* findings, immunofluorescence-labelled intestinal villi from mice fed with BoNT/A complex showed initial binding of BoNT/A starting at 2 h and peaked at 6 h. However, by 8 h, there is a decrease in immunofluorescence signal suggesting BoNT/A

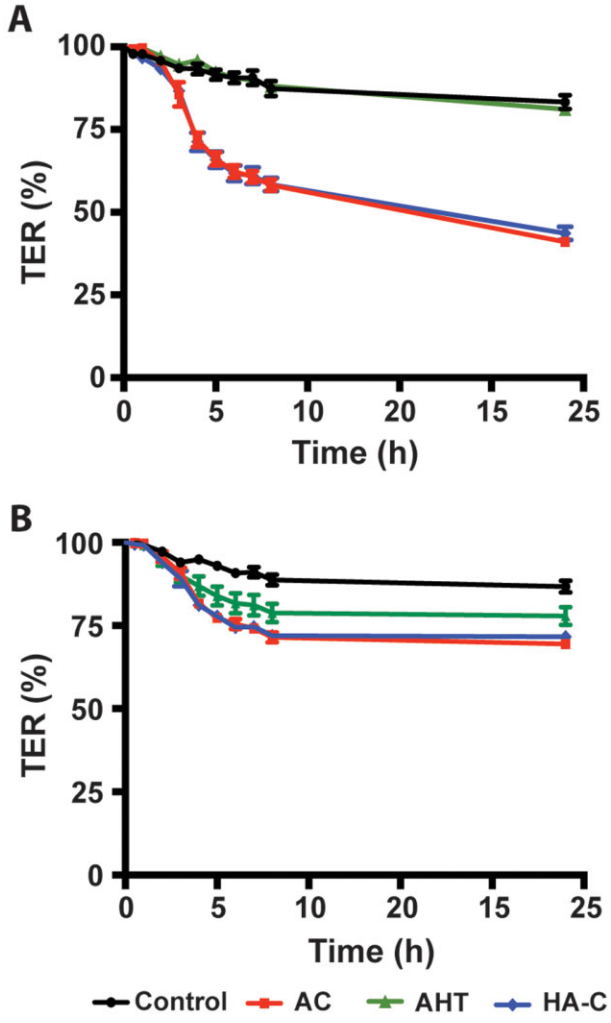

Fig. 3. Effects of BoNT/A complex, holotoxin and HA complex on transepithelial electrical resistance (TER). Caco-2 cell monolayers grown on permeable transwells were treated with 50 ng of BoNT/A complex (AC), 15 ng of BoNT/A holotoxin (AHT) or 20 ng of HA complex (HA-C) on the apical side (A) or the basolateral side (B). TER was measured over 24 h and expressed as percentage change in resistance at each data point from corresponding controls. Each data point represents an average of five independent experiments ± SEM. The background filter resistance was subtracted from the total electrical resistance across the monolayer.

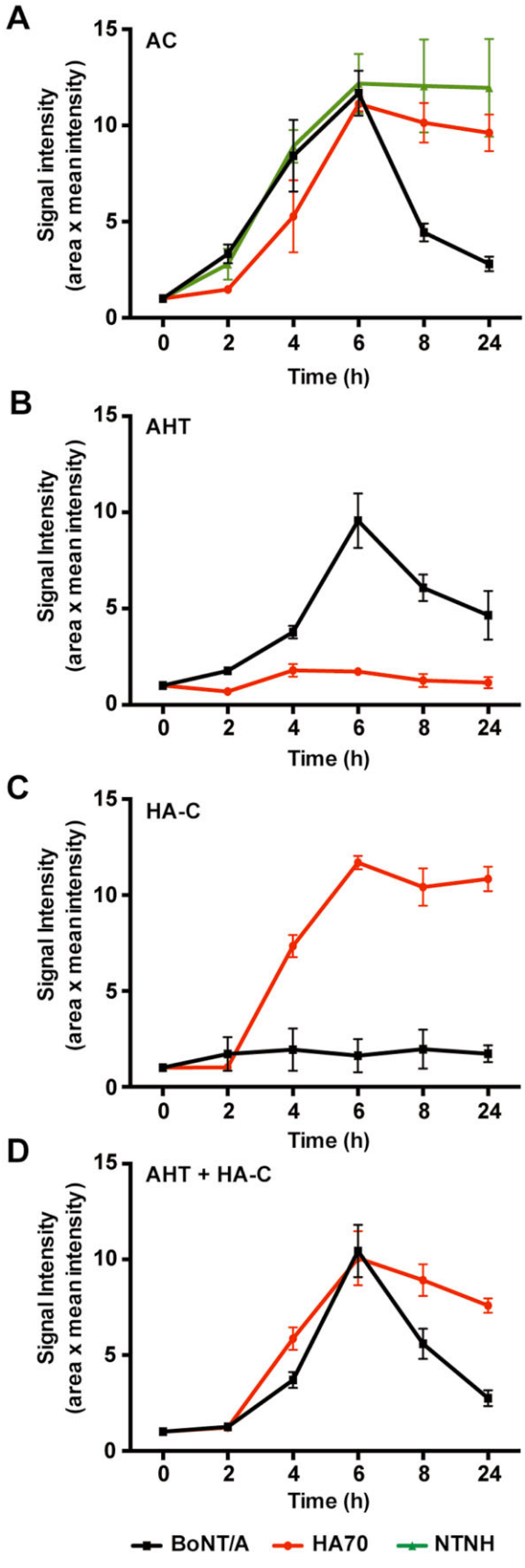

Fig. 4. Binding and translocation of BoNT/A, HA70 and NTNH through the mouse intestinal villi over time. Mice were given either BoNT/A complex (A), BoNT/A holotoxin (B), HA complex (C), or BoNT/A holotoxin and HA complex (D) by oral gavage. Segments of the upper small intestine were harvested over 24 h and labelled with a rabbit polyclonal antibody against BoNT/A, and mAbs against HA70 and NTNH. The immunofluorescence intensity was quantified by fluorescent thresholding using ImageJ software. Values represent mean signal intensities ± SEM ($n = 4$). Time 0 h represents control animals not treated with toxin or NAPs.

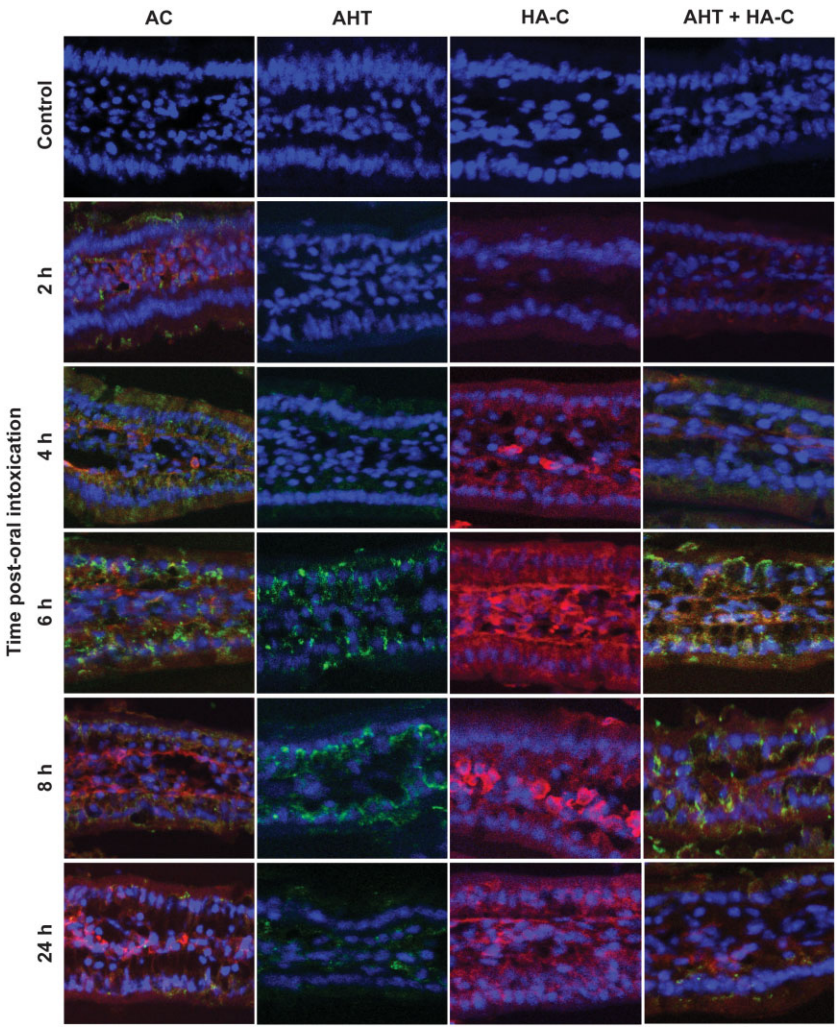

Fig. 5. Immunofluorescence tracking of the BoNT/A complex, BoNT/A holotoxin and HA complex entry through the mouse small intestinal villi. Representative confocal images of small intestinal villi sections harvested at 2, 4, 6, 8 and 24 h after oral gavage with BoNT/A complex (AC), BoNT/A holotoxin (AHT), HA complex (HA-C) or BoNT/A holotoxin with HA complex. Tissues were labelled with anti-BoNT/A (green) and HA70 (red). DAPI (blue) provided nuclear counterstaining. Images were shown at 40× magnification. ($n = 4$ mice per time point).

holotoxin clearance into the lymph or blood (Figs 4A and 5A). At the intestinal crypts, we found that BoNT/A complex started to appear at the crypts from 2 to 8 h and a decrease in toxin staining by 8 h (Supporting Information Fig. S6). The immunofluorescence signals for HA70 and NTNH showed initial binding that occurred at 2 h and plateaued after 6 h (Fig. 5A and Supporting Information Fig. S7), much like BoNT/A in the complex. Immunofluorescence-labelled intestinal villi from BoNT/A holotoxin fed with mice showed a significant binding that occurred at 4 h and peaked at 8 h. HA70 and NTNH were absent from BoNT/A holotoxin mice, as expected (Figs 4B and 5B). We also evaluated intestinal crypts from these tissues. Immunofluorescence images showed that holotoxin appeared in the crypts from 4 to 8 h with a decrease in immunostaining at 24 h (Supporting Information Fig. S6). Treatment of mice with the recombinant HA-C showed similar HA70 immunofluorescence pattern to BoNT/A complex, binding at 2 h and plateaued after 6 h with a longer sustained staining of HA70 at 24 h, suggesting that large amounts of HA70 remained bound to the intestinal cells (Figs 4C and 5C). Interestingly, the addition of BoNT/A holotoxin with HA-C did not enhance the time of BoNT/A appearance or binding in the small intestines to that seen in BoNT/A complex-treated mice (Fig. 5).

The binding and translocation of BoNT/A and NAPs was observed at the jejunum, ileum and colon sections (data not shown) but we focused on the upper portion of the small intestines of the duodenum as it is considered the primary site for toxin absorption (Sakaguchi, 1982).

Discussion

Botulinum neurotoxins have remarkable toxicity and are well adapted to entering the host where it targets neurons causing paralysis. Many questions regarding the oral route of intoxication remain, such as: How do BoNT complexes of potentially 900 kDa cross intestinal

epithelial barriers? What is the role of NAPs in the internalization of BoNT? Do holotoxins disassemble from toxin complexes?

What we know thus far from *in vivo* and *ex vivo* assays is that BoNT itself can transcytose across the intestinal epithelium (Fujinaga, 2010; Couesnon *et al*., 2012; Yao *et al*., 2014). Yet, there is a body of indirect and direct evidence which argues that the HA proteins in NAPs can interact with the intestinal epithelia. In one hypothesis, Fujinaga *et al*. proposed a three-step mechanism: (i) transcytosis, (ii) intestinal barrier disruption and (iii) entry of toxin through damaged epithelia (Fujinaga, 2010). The HAs bind mainly on the basolateral surface inducing loss of the paracellular barrier or cause cell damage, allowing toxin to move into the cells. HA33 was shown to facilitate transport of BoNT/D across epithelium and treatment with antibodies against HA70 and HA33 as well as incubation with sialic acid reduced cell binding and transport (Hasegawa *et al*., 2007). Recently, HA proteins were shown to interact with intestinal saccharides in a sialic acid or galactose-dependent process. Binding and transport were inhibited with anti-HA33 antibodies or the addition of saccharides (Ito *et al*., 2011). Although BoNT holotoxins alone can enter intestinal epithelial cells, NAPs play a role to facilitate its internalization.

In this study, we compared the internalization of BoNT/A holotoxin in the presence or absence of a recombinant HA-C with that of the BoNT/A complex. For the first time, the role of the NAPs in BoNT/A internalization was examined in both *in vivo* and *in vitro* models of intoxication. We showed that although BoNT/A holotoxin alone can translocate into Caco-2 cells (Fig. 2B, Supporting Information Figs S2–S4), there is a delay in toxin binding and entry (Fig. 2A). This delayed entry of BoNT/A holotoxin was also observed in the small intestines following oral intoxication in mice (Figs 4A and 5, Supporting Information Figs S5 and S6). When mice were treated with BoNT/A complex, there was binding of BoNT/A to the outer layers of the intestinal epithelia as early as 2 h and a gradual increase in BoNT/A staining in the lamina propria and intestinal crypts over time, peaking at 6 h post intoxication. Botulinum neurotoxin serotype A staining started to dissipate at about 8 h. These results correlated well with the *in vitro* Caco-2 internalization results (Fig. 2) as well as previous antibody protection results that showed mice fed with toxins and injected with neutralizing antibodies were only protected if antibodies were given by 6–7 h post oral intoxication (Cheng *et al*., 2009). In addition, toxin can be detected in the bloodstream starting at about 6 h, peaking at 7 h post oral intoxication, which coincided with the timing of BoNT/A signal decrease from the small intestines (Bagramyan *et al*., 2013). In these studies, BoNT/A holotoxin alone was observed to translocate across the small intestines in much the same way, except binding was visible starting at 4 h (2 h later than the BoNT/A complex) and peaked at 6–8 h.

Recombinantly purified HA-C comprising of an ~ 470 kDa complex with a stoichiometry of 3X HA70, 3X HA17 and 6X HA33 translocated into Caco-2 cells as well as the small intestine similar to the BoNT/A complex (Figs 2, 4 and 5). HA70 in the BoNT/A complex or HA-C, as well as NTNH in the BoNT/A complex, was observed to localize from the villi periphery into the inner lamina propria over time, and even prominently in the cell-like structures that are likely lymphatic immune cells (Fig. 5 and Supporting Information Fig. S5). Native gel analysis of purified BoNT/A complex showed that it consists of 88% of large-sized BoNT/A complexes and 7% of uncomplexed NTNH, and little uncomplexed NAPs (Cheng *et al*., 2008). It is unknown what condition the toxin complex would be in after digestion. Thus, the NAPs that remain in the intestines could be from excess NAPs in the toxin mixture or from those that have dissociated from the complex. Although we observed some co-localization of BoNT/A with HA70 and NTNH, there were far more NAPs or BoNT/A located independently of each other, suggesting that the toxin complex likely starts to disassemble before or following translocation through the epithelial cell layers (Fig. 5). Small amounts of BoNT/A and NAPs remain in the intestines after 24 h of intoxication, suggesting that depending on the amount of toxin ingested there may be a pool of toxin temporarily stored in intestinal cells. It is unclear why a pool of BoNT or NAPs persists in the intestines. Perhaps the translocation through membranes is inefficient or receptors for NAPs keep the accessory proteins in place. We report here a remarkable consistency of our results in both our *in vitro* and *in vivo* studies in the timing of BoNT uptake and internalization. Clearly, NAPs are not necessary for BoNT/A internalization, but do play a role in facilitating entry. For future studies, it would be worthwhile to explore how the persistence of toxins in the intestines could affect therapeutic efforts.

What role do NAPs play in translocation? Previous data suggested that NAPs, specifically HA33, can disrupt tight junctions, compromising the epithelial cell barrier and allowing BoNT complex to enter through a paracellular pathway (Fujinaga, 2010). The HA-C was also shown to bind E-cadherin, a cell adhesion protein that likely plays a major role in toxin cell surface binding (Sugawara *et al*., 2010; Lee *et al*., 2014). The HA-C was observed to disrupt membrane integrity (measured by TER) quickly after toxin or HA addition and much faster after addition of toxins or HA to the basolateral side. These data combined with the location of E-cadherin in the intercellular space suggested that the paracellular translocation pathway was the likely route for toxin complex entry (Lee *et al*., 2014). In contrast, our results from measuring TER of polarized

membranes of Caco-2 cell showed a gradual and mild disruption of membrane beginning at about 4 h after BoNT/A complex or HA-C addition to the apical side (Fig. 3A). When toxins were added to the basolateral side, an even smaller degree of membrane disruption was observed with BoNT/A complex compared with BoNT/A holotoxin (Fig. 3B). We did not observe obvious intestinal membrane disruptions in our small intestinal cross sections (Fig. 5). When BoNT/A holotoxin and the HA-C were added at the same time, no increase in the timing of BoNT/A holotoxin translocation to Caco-2 or small intestinal villi was observed (Fig. 2D and Supporting Information Fig. S5). Thus, in the absence of the NTNH link between the HA-C and BoNT/A holotoxin, toxin entry was not facilitated through a paracellular pathway of transport. The slight membrane disruption observed in TER reductions probably led to some paracellular translocation of the toxin but was likely not the main contributor to BoNT/A translocation. However, despite our results, we believe both models (paracellular vs. receptor-mediated internalization) are possible depending on the amount of toxins present. In the previous TER model, when in the presence of high levels of BoNT toxins, the predominant mode of transport is the likely paracellular pathway mediated by E-cadherin disruption of tight junctions. Our TER assays use substantially less toxin or HA protein than other assays and thus we do not observe the obvious effect of tight junction disruption.

Recent studies showed the intestinal cell internalization of *Listeria monocytogenes* via an E-cadherin mediated pathway at multicellular junctions formed when senescent intestinal cells are expelled and detached by extrusion and from goblet cells. *Listeria monocytogenes* did not disrupt tight cellular junctions but exploited the binding of its surface proteins internalin A and B with E-cadherin to facilitate binding and endocytosis (Pentecost *et al*., 2006; 2010; Nikitas *et al*., 2011). Similar pathways may be exploited by the BoNT complex for intestinal entry.

Our results also contrast with *ex vivo* studies where upper intestinal sections were treated with fluorescent-labelled BoNT/A heavy chain at 4°C for 30–120 min (Couesnon *et al*., 2012). These studies showed that the entry site for the heavy chain domain of BoNT/A is predominantly located in the intestinal crypt cells, and then targets the submucosa and musculosa neurons. Yao *et al*. also showed in *ex vivo* studies that NAPs bind to the small intestines and that the binding was likely through the interaction between HA70 and HA33 with host carbohydrates (Yao *et al*., 2014). Using this model, they did not observe any holotoxin binding but that was likely because of the short exposure time (30 min). Toxin entry could be interrupted with the addition of receptor-mimicking saccharides suggesting an HA-mediated receptor-mediated entry pathway (Couesnon *et al*., 2012; Yao *et al*., 2014). Using our live mouse experiments, we were able to test the *in vivo* uptake of BoNT/A holotoxin, BoNT/A complex and a recombinantly derived HA-C over 24 h. Uptake was observed in intestinal villi as well as crypts. The longer exposure of the animals with toxin allowed for comparison of uptake of the holotoxin vs. BoNT/A complex, as well as the contribution of the HA-C. In summary, we propose that the BoNT/A complex can be internalized first through the interactions of the HA-C with epithelial cell receptors, likely surface oligosaccharides, and second through interaction of the BoNT/A holotoxin with its own cell receptors. Under low toxin levels, such as after digestion processing through the stomach and intestines, the paracellular transport pathway likely did not play a significant role in BoNT/A complex translocation.

Some BoNT subtypes (such as BoNT/A2 and BoNT/A3) and BoNT/E toxin complexes contain alternate, non-HA-type NAPs such as OrfXs, p21 or p47 (Hill *et al*., 2007). How these NAPs contribute to toxicity differences, and how well mouse oral bioavailability data translate to human oral intoxication remain to be explored. A better understanding of how large toxin complexes traverse the intestinal epithelia could lead to a better understanding of toxin-mediated pathogenesis. Because BoNTs are also currently explored as vehicles for neuronal oral drug delivery, this could lead to the design and delivery of orally delivered drugs for a multitude of diseases.

Experimental procedures

Materials

Botulinum neurotoxin serotype A holotoxin, BoNT/A complex and rabbit polyclonal antibodies against BoNT/A were purchased from Metabiologics. The median lethal dose of BoNT/A holotoxin and complex was estimated at 0.42 ng kg^{-1} or about 8 pg/mouse by intraperitoneal injection and 27 μg kg^{-1} or about 0.5 μg/mouse for BoNT/A complex via oral gavage (Cheng *et al*., 2008). Caco-2, a human epithelial colon adenocarcinoma cell line, was purchased from the American Type Culture Collection. Chemicals and reagents were purchased from Sigma-Aldrich and tissue culture supplies were from Life Technologies. Monoclonal antibodies (mAbs): a mAb against the NTNH complex protein, referred to as NTNH 84-27-7-5, was generated following immunization with a recombinant protein corresponding to aa 616-1193 of the NTNH molecule and prepared in Phosphate Buffered Saline (PBS) by the Stanker laboratory (unpublished results); the HA70 specific mAb, NAP80-7-2-1 (Stanker *et al*., 2013). The recombinant HA-C was obtained from the Jin lab and was prepared as described in Lee *et al*. 2013 (Gu *et al*., 2012; Lee *et al*., 2013).

Animals

Female Swiss Webster mice (4–5 weeks old, 20–25 g) were purchased from Charles River Laboratories. All animals were

housed in the small animal facility at the USDA under standard housing conditions and generally allowed unrestricted access to food and water. All procedures involving animals were reviewed and approved by the Institutional Animal Care and Use Committee of the United States Department of Agriculture, Western Regional Research Center.

Cell culture

Caco-2 cells (ATCC) were grown on 25 mm glass coverslips and maintained in Dulbecco's modified Eagle's medium supplemented with 10% fetal bovine serum, 1% non-essential amino acids, 0.01 mg ml^{-1} of human transferrin, 10 000 U of penicillin per ml, and 10 ng of streptomycin per ml in an atmosphere of 95% air-5% CO_2. On the day of experiments, Caco-2 cells were washed in HBSS and treated either with 15 ng ml^{-1} (100 pM), 50 ng ml^{-1} (56 pM), or 20 ng ml^{-1} (43 pM) of BoNT/A holotoxin, BoNT/A complex or recombinant HA-C, prepared in HBSS. For antibody evaluation and for visualization of toxin binding, cells were incubated with BoNT/A holotoxin and complex for 4 h. In separate experiments, Caco-2 cells were treated with BoNT/A toxins in the presence or absence of the HA-C for only 1 h to evaluate the time required for toxin binding and internalization. After incubation, unbounded toxins and associated proteins were removed with 1X HBSS and cells were incubated in 1X HBSS. Coverslips containing cells were removed at 4 h (Fig. 1) or at indicated times of 0, 2, 4, 6, 8 and 24 h after toxin or HA-C treatment (Fig. 2). Cells in coverslips were then fixed in 4% paraformaldehyde (PFA) for 10 min and rinsed with 1X PBS before immunofluorescence staining.

Immunofluorescence staining

Double immunostaining was performed with either confluent Caco-2 monolayers on glass coverslips or small intestinal cryosections that were rinsed twice with PBS and permeabilized with 1% triton X-100 in PBS for 30 min. Samples were incubated with blocking solution (2% goat serum, 0.2% Triton X-100 and 0.1% Bovine Serum Albumin) for 1 h, and then incubated with 1:250 blocking buffer diluted solutions of a polyclonal rabbit antibody against BoNT/A (2 mg ml^{-1} of stock), and mAbs against either HA70 (1.6 mg ml^{-1} of stock) or NTNH (5.5 mg ml^{-1} of stock). After washing three times, cells or tissue were incubated with Alexa Fluor 488 to mouse IgG or Alexa Fluor 568 to rabbit IgG (1:500 dilution; Life Technologies) and mounted onto glass slides using the hard-set DAPI mounting medium (Vector Laboratories). Florescence signals were visualized with a Leica Microsystems confocal microscope (Leica TCS SP5) with the appropriate filter sets. For analysis of BoNT/A and HA70 internalization into the intestinal epithelial cells, total fluorescence intensity was quantified in at least 81 optical fields taken from three independent experiments. For quantification, the mean fluorescence was measured in three randomly selected non-overlapping 40x fields with each containing approximately 100–150 Caco-2 cells. Similarly, the mean fluorescence of the small intestinal tissue sections was measured in four separate 40x fields per animal in each time point. Raw fluorescence was then normalized to control levels and the percent increase in fluorescence was calculated from these normalized values. Negative controls were prepared by omitting the primary antibodies.

Determination of transepithelial resistance (TER)

Caco-2 cells were grown on rat-tail collagen-coated Millicell Cell Culture Inserts (growth area 0.6 cm^2, pore size 0.4 μm) at a cell density of approximately 10^5 cells/cm^2. Filters with cell monolayers were used at 14 days after seeding. Transepithelial electrical resistance was measured using a volt-ohm meter (World Precision Instruments). All TER experiments were conducted in 0.4 and 0.6 ml of HBSS without phenol red (Gibco, Life technologies) in the apical and basolateral reservoirs, respectively. Up to 15 ng ml^{-1} of BoNT/A holotoxin, 50 ng ml^{-1} of BoNT/A complex or 20 ng ml^{-1} of recombinant HA-C were added to either the apical or basolateral reservoirs and incubated with cells for the duration of the experiment. Only filters with an initial resistance of ≥ 300 Ω cm^2 were used. For analysis of independent experiments, results were expressed as percentages of the corresponding control resistance of each dataset.

Small intestine cryosections

Mice were administered 0.6, 2 or 0.8 μg/mouse, respectively, of phosphate gelatin (0.028 M sodium phosphate, pH 6.2 and 0.2% gelatin) diluted BoNT/A holotoxin, complex and recombinant HA70 complex by gavage with popper feeding needles directly into the vicinity of mouse stomachs. At 2, 3, 4, 6, 7, 8 and 24 h post intoxication, three mice per time point were euthanized and perfusion-fixed with normal saline followed by 4% PFA. Control mice were orally treated with phosphate gelatin for 6 h. Segments of the small intestine were immersed in 4% PFA overnight, cryoprotected with 20% sucrose for 2 days, embedded in OCT embedding medium (Tissue-Tek, Miles Laboratories) and stored at −80°C. Cryosections (5 μm) were cut with a cryostat microtome and mounted onto SuperFrost glass slides (Fisher Scientific).

Statistical analyses

For *in vivo* studies, four mice were used per time point. For cell culture studies, n = number of independent experiments, each independent experiment contained triplicated culture wells or glass coverslips of each study condition. All data were expressed as mean ± standard error of the mean and assessed using one-way ANOVA followed by the Tukey–Kramer test where multiple groups are compared, and P-values < 0.05 are taken to indicate significance differences between groups.

Acknowledgements

The authors would like to acknowledge Drs. Kirkwood Land, Xiaohua He and Wallace Yokoyama for their helpful comments; Wanless Hatcher, Zeke Martinez and Jacqueline Miller for their help with animal care and handling. This work was funded by the United States Department of Agriculture, Agricultural Research Service, National Program Project NP108, CRIS 5325-42000-048-00D. L.W.C. and R.J. were also funded by the National Institute of Allergy and Infectious Diseases Service Grant U54 AI065359 and RO1A1091823, respectively. L.H.S. was also funded by Interagency Agreement IAA#40768.

References

Ahsan, C.R., Hajnoczky, G., Maksymowych, A.B., and Simpson, L.L. (2005) Visualization of binding and

transcytosis of botulinum toxin by human intestinal epithelial cells. *J Pharmacol Exp Ther* **315:** 1028–1035.
Al-Saleem, F.H., Ancharski, D.M., Joshi, S.G., Elias, M., Singh, A., Nasser, Z., and Simpson, L.L. (2012) Analysis of the mechanisms that underlie absorption of botulinum toxin by the inhalation route. *Infect Immun* **80:** 4133–4142.
Arnon, S.S., Schechter, R., Inglesby, T.V., Henderson, D.A., Bartlett, J.G., Ascher, M.S., *et al.* (2001) Botulinum toxin as a biological weapon: medical and public health management. *JAMA* **285:** 1059–1070.
Bagramyan, K., Kaplan, B.E., Cheng, L.W., Strotmeier, J., Rummel, A., and Kalkum, M. (2013) Substrates and controls for the quantitative detection of active botulinum neurotoxin in protease-containing samples. *Anal Chem* **85:** 5569–5576.
Barash, J.R., and Arnon, S.S. (2014) A novel strain of *Clostridium botulinum* that produces type B and type H botulinum toxins. *J Infect Dis* **209:** 183–191.
Bigalke, H., and Rummel, A. (2005) Medical aspects of toxin weapons. *Toxicology* **214:** 210–220.
Chen, F., Kuziemko, G.M., and Stevens, R.C. (1998) Biophysical characterization of the stability of the 150-kilodalton botulinum toxin, the nontoxic component, and the 900-kilodalton botulinum toxin complex species. *Infect Immun* **66:** 2420–2425.
Cheng, L.W., Onisko, B., Johnson, E.A., Reader, J.R., Griffey, S.M., Larson, A.E., *et al.* (2008) Effects of purification on the bioavailability of botulinum neurotoxin type A. *Toxicology* **249:** 123–129.
Cheng, L.W., Stanker, L.H., Henderson, T.D., 2nd, Lou, J., and Marks, J.D. (2009) Antibody protection against botulinum neurotoxin intoxication in mice. *Infect Immun* **77:** 4305–4313.
Couesnon, A., Molgo, J., Connan, C., and Popoff, M.R. (2012) Preferential entry of botulinum neurotoxin A Hc domain through intestinal crypt cells and targeting to cholinergic neurons of the mouse intestine. *PLoS Pathog* **8:** e1002583.
Eisele, K.H., Fink, K., Vey, M., and Taylor, H.V. (2011) Studies on the dissociation of botulinum neurotoxin type A complexes. *Toxicon* **57:** 555–565.
Fujinaga, Y. (2010) Interaction of botulinum toxin with the epithelial barrier. *J Biomed Biotechnol* **2010:** 974943.
Fujinaga, Y., Matsumura, T., Jin, Y., Takegahara, Y., and Sugawara, Y. (2009) A novel function of botulinum toxin-associated proteins: HA proteins disrupt intestinal epithelial barrier to increase toxin absorption. *Toxicon* **54:** 583–586.
Gu, S., Rumpel, S., Zhou, J., Strotmeier, J., Bigalke, H., Perry, K., *et al.* (2012) Botulinum neurotoxin is shielded by NTNHA in an interlocked complex. *Science* **335:** 977–981.
Hasegawa, K., Watanabe, T., Suzuki, T., Yamano, A., Oikawa, T., Sato, Y., *et al.* (2007) A novel subunit structure of *Clostridium botulinum* serotype D toxin complex with three extended arms. *J Biol Chem* **282:** 24777–24783.
Hill, K.K., Smith, T.J., Helma, C.H., Ticknor, L.O., Foley, B.T., Svensson, R.T., *et al.* (2007) Genetic diversity among botulinum neurotoxin-producing clostridial strains. *J Bacteriol* **189:** 818–832.
Hines, H.B., Lebeda, F., Hale, M., and Brueggemann, E.E. (2005) Characterization of botulinum progenitor toxins by mass spectrometry. *Appl Environ Microbiol* **71:** 4478–4486.
Inoue, K., Fujinaga, Y., Watanabe, T., Ohyama, T., Takeshi, K., Moriishi, K., *et al.* (1996) Molecular composition of *Clostridium botulinum* type A progenitor toxins. *Infect Immun* **64:** 1589–1594.
Ito, H., Sagane, Y., Miyata, K., Inui, K., Matsuo, T., Horiuchi, R., *et al.* (2011) HA-33 facilitates transport of the serotype D botulinum toxin across a rat intestinal epithelial cell monolayer. *FEMS Immunol Med Microbiol* **61:** 323–331.
Jin, Y., Takegahara, Y., Sugawara, Y., Matsumura, T., and Fujinaga, Y. (2009) Disruption of the epithelial barrier by botulinum haemagglutinin (HA) proteins – differences in cell tropism and the mechanism of action between HA proteins of types A or B, and HA proteins of type C. *Microbiology* **155:** 35–45.
Lee, K., Gu, S., Jin, L., Le, T.T., Cheng, L.W., Strotmeier, J., *et al.* (2013) Structure of a bimodular botulinum neurotoxin complex provides insights into its oral toxicity. *PLoS Pathog* **9:** e1003690.
Lee, K., Zhong, X., Gu, S., Kruel, A.M., Dorner, M.B., Perry, K., *et al.* (2014) Molecular basis for disruption of E-cadherin adhesion by botulinum neurotoxin A complex. *Science* **344:** 1405–1410.
Maksymowych, A.B., and Simpson, L.L. (1998) Binding and transcytosis of botulinum neurotoxin by polarized human colon carcinoma cells. *J Biol Chem* **273:** 21950–21957.
Maksymowych, A.B., and Simpson, L.L. (2004) Structural features of the botulinum neurotoxin molecule that govern binding and transcytosis across polarized human intestinal epithelial cells. *J Pharmacol Exp Ther* **310:** 633–641.
Maksymowych, A.B., Reinhard, M., Malizio, C.J., Goodnough, M.C., Johnson, E.A., and Simpson, L.L. (1999) Pure botulinum neurotoxin is absorbed from the stomach and small intestine and produces peripheral neuromuscular blockade. *Infect Immun* **67:** 4708–4712.
Matsumura, T., Jin, Y., Kabumoto, Y., Takegahara, Y., Oguma, K., Lencer, W.I., and Fujinaga, Y. (2008) The HA proteins of botulinum toxin disrupt intestinal epithelial intercellular junctions to increase toxin absorption. *Cell Microbiol* **10:** 355–364.
Montecucco, C., and Schiavo, G. (1994) Mechanism of action of tetanus and botulinum neurotoxins. *Mol Microbiol* **13:** 1–8.
Montecucco, C., Papini, E., and Schiavo, G. (1996) Bacterial protein toxins and cell vesicle trafficking. *Experientia* **52:** 1026–1032.
Nikitas, G., Deschamps, C., Disson, O., Niault, T., Cossart, P., and Lecuit, M. (2011) Transcytosis of *Listeria monocytogenes* across the intestinal barrier upon specific targeting of goblet cell accessible E-cadherin. *J Exp Med* **11:** 2263–2277.
Ohishi, I., Sugii, S., and Sakaguchi, G. (1977) Oral toxicities of *Clostridium botulinum* toxins in response to molecular size. *Infect Immun* **16:** 107–109.
Pentecost, M., Otto, G., Theriot, J.A., and Amieva, M.R. (2006) *Listeria monocytogenes* invades the epithelial junctions at sites of cell extrusion. *PLoS Pathog* **2:** e3.
Pentecost, M., Kumaran, J., Ghosh, P., and Amieva, M.R.

(2010) *Listeria monocytogenes* invades the epithelial junctions at sites of cell extrusion. *PLoS Pathog* **6:** e1000900.
Sakaguchi, G. (1982) Clostridium botulinum toxins. *Pharmacol Ther* **19:** 165–194.
Scarlatos, A., Welt, B.A., Cooper, B.Y., Archer, D., DeMarse, T., and Chau, K.V. (2005) Methods for detecting botulinum toxin with applicability to screening foods against biological terrorist attacks. *J Food Sci* **70:** 121–130.
Schiavo, G., Santucci, A., Dasgupta, B.R., Mehta, P.P., Jontes, J., Benfenati, F., *et al*. (1993) Botulinum neurotoxins serotypes A and E cleave SNAP-25 at distinct COOH-terminal peptide bonds. *FEBS Lett* **335:** 99–103.
Simpson, L. (2013) The life history of a botulinum toxin molecule. *Toxicon* **68:** 40–59.
Stanker, L.H., Scotcher, M.C., Cheng, L., Ching, K., McGarvey, J., Hodge, D., and Hnasko, R. (2013) A monoclonal antibody based capture ELISA for botulinum neurotoxin serotype B: toxin detection in food. *Toxins* **5:** 2212–2226.
Sugawara, Y., Matsumura, T., Takegahara, Y., Jin, Y., Tsukasaki, Y., Takeichi, M., and Fujinaga, Y. (2010) Botulinum hemagglutinin disrupts the intercellular epithelial barrier by directly binding E-cadherin. *J Cell Biol* **189:** 691–700.
Sugii, S., Ohishi, I., and Sakaguchi, G. (1977) Correlation between oral toxicity and in vitro stability of *Clostridium botulinum* type A and B toxins of different molecular sizes. *Infect Immun* **16:** 910–914.
Yao, G., Lee, K., Gu, S., Lam, K.H., and Jin, R. (2014) Botulinum neurotoxin A complex recognizes host carbohydrates through its hemagglutinin component. *Toxins* **6:** 624–635.

Supporting information

Additional Supporting Information may be found in the online version of this article at the publisher's web-site:

Fig. S1. Western blots analysis of BoNT/A complex and NAPs (HA70 and NTNH). Each lane contains 2 μg of BoNT/A complex treated with 10 mM DTT (even numbered lanes) or without (odd numbered lanes). Samples were run on 4–12% SDS-PAGE and transferred to a PVDF membrane. Lanes 1, 2 show Coomassie blue stained samples. Lanes 3, 4 were probed with anti-NTNH mAb; lanes 5, 6 were probed with a rabbit polyclonal anti-BoNT/A; and lanes 7, 8 were probed with anti-HA70 mAb. MW: protein molecular weight markers (kDa).

Fig. S2. Confocal Z stack videos of BoNT/A complex (A) and holotoxin (B) translocation. Z stack optical images were gathered to demonstrate BoNT/A complex (AC) and holotoxin (AHT) distribution throughout the Caco-2 cell monolayer. Caco-2 cell monolayer exposed to BoNT/A complex (video 1) or holotoxin (video 2) for 4 h and stained with Alexa-488 BoNT/A (green), Alexa-568 HA70 (red) and DAPI (nuclei stain, blue). Videos illustrate transcytosis of BoNT/A complex and holotoxin across the Caco-2 monolayer and not just binding to the cell surface.

Fig. S3. Internalization of BoNT/A holotoxin, BoNT/A complex into Caco-2 cells. (A) Caco-2 cells were treated with media (control) or with BoNT/A complex (AC), holotoxin (AHT) for 4 h at 37°C. Cells were stained with of Alexa-488 labelled antibodies against BoNT/A (green), phalloidin (red) and DAPI (blue). Cells were viewed under 40× magnification. (B) Zoomed-in view of Caco-2 cells treated with BoNT/A complex. (C) Zoomed-in view of Caco-2 cells treated with BoNT/A holotoxin.

Fig. S4. BoNT/A staining in Caco-2 cells treated with complex (AC) and holotoxin (AHT). Cells were stained with rabbit anti-BoNT/A followed with goat anti-rabbit Alexa 488 (green) and DAPI (blue) and viewed under 63× magnification.

Fig. S5. Translocation of BoNT/A complex, BoNT/A holotoxin and HA complex through the mouse intestinal villi. Representative confocal images of frozen sections of small intestinal villi illustrate the binding and internalization of BoNT/A (green) and HA70 (red) through the mouse intestinal epithelia. DAPI (blue) provides nuclear counterstaining. Samples were imaged at 40×, $n = 4$ mice per time point.

Fig. S6. Staining of BoNT/A complex, BoNT/A holotoxin and HA70 in the mouse intestinal crypts. Representative confocal images illustrate anti-BoNT/A (green) and HA70 (red) binding to intestinal crypts. Samples were imaged at 40×, $n = 4$ mice per time point.

Fig. S7. Translocation of BoNT/A complex through the mouse intestinal villi. Representative confocal images of frozen sections of small intestinal villi illustrate the binding and internalization of BoNT/A (green) and NTNH (red) through the mouse intestinal epithelia. DAPI (blue) provides nuclear counterstaining. Samples were imaged at 40× (left panel) and further magnified 10× (right panel), $n = 4$ mice per time point.

